

An Evaluation of Soil Moisture Retrievals Using Aircraft and Satellite Passive Microwave Observations during SMEX02

John D. Bolten¹ and Venkat Lakshmi²

¹Hydrological Sciences Branch
NASA/Goddard Space Flight Center
Greenbelt, MD 20771
john.bolten@nasa.gov

²Department of Geological Sciences
University of South Carolina, Columbia SC 29208
vlakshmi@geol.sc.edu

Abstract

The Soil Moisture Experiments conducted in Iowa in the summer of 2002 (SMEX02) had many remote sensing instruments that were used to study the spatial and temporal variability of soil moisture. The sensors used in this paper (a subset of the suite of sensors) are the AQUA satellite-based AMSR-E (Advanced Microwave Scanning Radiometer- Earth Observing System) and the aircraft-based PSR (Polarimetric Scanning Radiometer). The SMEX02 design focused on the collection of near simultaneous brightness temperature observations from each of these instruments and in situ soil moisture measurements at field- and domain- scale. This methodology provided a basis for a quantitative analysis of the soil moisture remote sensing potential of each instrument using in situ comparisons and retrieved soil moisture estimates through the application of a radiative transfer model. To this end, the two sensors are compared with respect to their estimation of soil moisture.

Key words: remote sensing, soil moisture, microwave, field experiment, passive

1. Introduction

Many studies have shown the importance of soil moisture in the realm of agriculture, hydrology and climatology by demonstrating the influence of soil moisture dynamics on surface runoff, infiltration, heat flux and local climate. Observations are needed at all scales for hydrologic modeling, weather forecasting, climate prediction, flood and drought monitoring and other water and energy cycle applications. However, soil moisture varies in space and time. The resulting heterogeneous nature of near surface soil moisture makes accurate point measurements at high spatial and temporal scales difficult. The utilization of remote sensing may enable a better understanding of these boundary condition relationships and land-surface hydrologic processes.

Previous studies¹⁾²⁾ have demonstrated the strong relationship between microwave brightness temperature T_B and near surface soil moisture over bare and moderately vegetated ($<5 \text{ kg/m}^2$ water content) surfaces. These advances have led to the current state of large-scale soil moisture observation using aircraft and satellite-based instruments. However, less work has focused on the comparison of soil moisture estimates from multiple frequencies and spatial resolutions. Of particular interest are the ambiguities associated with the upscaling of field data and airborne observations to space-borne radiometer footprints. Scale complexities must be considered when testing the application of soil moisture retrieval algorithms. Examining simultaneous observations (multi-frequency in the microwave spectrum) of remotely sensed soil moisture at multiple scales is a critical benchmark for evaluating the value of such observations and will lead to a better understanding of heterogeneity effects and sensor

accuracy.

In this paper, an evaluation of concurrent passive microwave observations from aircraft and space-borne sensors during the Soil Moisture Experiments 2002 (SMEX02) is presented. Brightness temperatures from the satellite-based Earth Observing System (EOS) Advanced Microwave Scanning Radiometer (AMSR-E) and the airborne C- and X-band Polarimetric Scanning Radiometer (PSR C/X) are incorporated into an iterative, least-squares soil moisture retrieval algorithm utilizing a single-channel microwave emission model. Aggregation of the finer resolution PSR C/X brightness temperatures to AMSR-E resolution is performed in order to provide a more accurate comparison of the two instruments. Thus, daily soil moisture estimates for the SMEX02 region at the 50 km resolution of the AMSR-E instrument are produced. The utility of AMSR-E and PSR C/X for near surface soil moisture retrieval is then evaluated against ground-based soil moisture measurements collected during the experiment. The goal is to quantify the differences in soil moisture sensitivity of each instrument. Such a difference in spatial resolution presents a unique opportunity to investigate the linear scaling of observed and modeled brightness temperatures and assess the applied algorithm at each scale.

Previous studies using SMEX02 data have involved the analysis of AMSR-E and PSR C/X brightness temperatures mostly at the field-scale and watershed-scale. These studies mainly focused on the application of hydrometeorological data³⁾ and field-scale moisture validation⁴⁾ within the Walnut Creek Watershed. This manuscript continues these investigations by quantitatively comparing the modeled and observed satellite-scale X-band T_B from each instrument in order to assess the effects of frequency, scale, and footprint heterogeneity on moisture prediction. By applying the observed brightness

temperatures from both instruments to a common retrieval algorithm, the performance of each instrument is possible. We present a statistical analysis of the remote sensing and biophysical parameters during SMEX02 to gain a better understanding of these inter-related factors.

2. SMEX02 Field Experiment: data and methods

SMEX02 was designed to combine field sampling and simultaneous remote sensing observations to study the effects of soil moisture and field-scale heterogeneity on land-atmosphere fluxes. The duration of the experiment was June 25th to July 12th, 2002; during which a series of thunderstorms occurred on July 4th, July 7th and July 10th which provided large changes in soil moisture for the analysis of remote sensing observations. A major element of SMEX02 was daily passive microwave airborne support for AMSR-E algorithm development and validation. The sampling protocol was designed to provide a daily average surface volumetric soil moisture value at a scale equivalent to two spaceborne AMSR-E footprints, approximately 50 km x 100 km. This consisted of daily ground sampling from 47 individual field sites spaced over the study area. Each site is located in an agricultural field which is normally a quarter section, or 800 m by 800 m. Efforts were made to sample the entire region as close in time to the AMSR-E ascending overpass (1330 local time) as possible. In addition, the PSR C/X was flown as close in time to the AMSR-E overpass and in situ sampling times as possible, between the 1200 and 1500 local time. Dual-polarized brightness temperature data collected during the study were analyzed with an emphasis on the differences in spatial resolution of the two instruments: ~56 km for AMSR-E and 2 km

for PSR C/X, respectively.

Field data collection during SMEX02 included observations of volumetric and gravimetric soil moisture, air temperature, soil temperature, bulk density, surface roughness, vegetation water content, and crop type. The primary soil moisture measurements at the regional sites consisted of three capacitance probe samples for the 0-6 cm surface layer and one gravimetric soil moisture measurement at depths of 0-1 cm and 0-6 cm.

Approximately 95% of the SMEX02 region comprises of row crop agriculture, a majority of this being corn (50%), soybean (40-45%), and the remaining 5-10% being forage and grains. During the study the soybean fields grew from essentially bare soils to vegetation water content w_c , of 1-1.5 kg/m² while the corn fields increased from 2-3 kg/m² to 4-5 kg/m². Crop specific relationships between Landsat Normalized Difference Water Index (NDWI) and w_c were established to provide an extensive mapping of vegetation parameters over the study area as described in⁵⁾. A more detailed description of the SMEX02 field campaign and methodology can be found at [<http://hydrolab.arsusda.gov/smex02>].

2.1 Advanced Microwave Scanning Radiometer for EOS (AMSR-E)

The Advanced Microwave Scanning Radiometer for EOS (AMSR-E) is a passive microwave radiometer system mounted on the NASA EOS *Aqua* satellite⁶⁾. It measures brightness temperatures at 6.9, 10.7, 18.7, 23.8, 36.5, and 89.0 GHz, with vertical and horizontal polarizations at each frequency. The instrument has a fixed incidence angle of 55° and ranges in mean footprint diameters from 56 km at 6.92 GHz to 5 km at 89 GHz.

Ten days of the AMSR-E Level-2A (AE_L2A), ascending data (June 25, July 1, 2, 4, 6, 7, 8, 9, 10, 11) acquired from the National Snow and Ice Data Center (NSIDC) are used in this study. The AMSR-E 6.925 GHz channels observed notable RFI interference in portions of the SMEX02 domain, particularly near Des Moines, IA located in the southwestern portion of the study area. However, little RFI was observed in the other AMSR-E channels; therefore, brightness temperatures from the X-band 10.7 GHz AMSR-E channels are used exclusively in this analysis.

2.2 Polarimetric Scanning Radiometer Instrument (PSR C/X)

The PSR C/X is a passive airborne microwave imaging radiometer system developed for the purpose of obtaining high-resolution multi-band polarimetric emission imagery⁷⁾. PSR C/X provides simultaneous vertical and horizontal polarized measurements within 8 frequency bands ranging from 6.00-10.75 GHz. The center frequencies for the C- and X-bands are 6.00, 6.50, 6.92, 7.32, 10.64, 10.69, 10.70, 10.75 GHz. Only the 10.70 GHz channel was used in this analysis due to low occurrences of radio frequency interference (RFI) at this frequency, and also to match the AMSR-E X-band. The instrument was flown over four regional flight lines at altitudes of ~1500 m and ~8000 m respectively, with a conical scanning mode at an observation angle of 55°. These flight patterns were performed for ten days of the study (June 25, 27, 29 and July 1, 4, 8, 9, 10, 11, 12), seven of which correspond to AMSR-E ascending overpasses and ground sampling. In the current analysis only the high altitude data were used, i.e., a swath width of 25.5 km and an average footprint size of 2.3 km at 10.7 GHz.

2.3. Co-location and comparison techniques

The SMEX02 experiment design facilitated data comparison at the AMSR-E footprint-scale (~50 km). To properly evaluate the soil moisture retrievals from AMSR-E and PSR using field observations and measurements from each instrument, we carefully co-located all observations and up-scaled the ground and PSR C/X observations to produce comparable estimates of regional soil moisture (i.e., AMSR-E footprint scale). Estimates of remote sensing observations and the corresponding in-situ observations were calculated by averaging brightness temperatures and soil moisture estimates that were located completely within the extent of each AMSR-E footprint. It was necessary to assume a linear scaling of the radiometric data and ground observations (i.e. we are using averaging) however we recognize that this may introduce some uncertainty into the analyses. As shown in McCabe et al.³⁾, resampling of PSR C/X brightness temperatures to a number of coarser resolutions (up to 25 km) yield statistical consistency, giving confidence in upscaling PSR C/X data for sensor intercomparison. Averaging of the point measurements and PSR C/X data to AMSR-E resolution facilitated two satellite-scale values within the SMEX02 domain for each day of concurrent observations. Thus, two AMSR-E brightness temperature means were calculated from the over-sampled footprints centers (approximately 12 densely sampled footprints) within the SMEX02 domain for each day of observations. In order to limit radiometric influences from outside of the SMEX02 domain, only radiometer footprints that were located entirely within the SMEX02 region were used. The central purpose of this analysis is to incorporate all (i.e., field, PSR C/X, AMSR-E) observations into a microwave emission model in order to produce comparable estimates of regional soil moisture. This framework is envisaged to illustrate

satellite-scale brightness temperature and soil moisture relationships, and gauge the effectiveness of the soil moisture retrieval algorithm.

3. Results

Prior to our evaluation, a sensitivity analysis of AMSR-E and PSR X-band T_B observations with 0-1 cm and 0-6 cm in situ soil moisture measurements was performed. A regression analysis was completed using both the 0-1 cm and 0-6 cm in situ soil moisture data to establish a correlation with observed brightness temperature for both the AMSR-E and PSR C/X instruments. The 0-1 cm data were shown to have a higher correlation with X-band observations. This supports previous studies estimating the X-band penetration depth being a few mm. Therefore, the 0-1 cm soil moisture measurements were used for the following analysis; the modeled brightness temperatures and estimated soil moistures are assumed to represent the 0-1 cm soil layer in this study. These results are summarized in Table 1.

Both observed brightness temperatures and estimated soil moistures were influenced by changes in vegetation water content and soil wetness during the experiment. It is important to note that the range of vegetation water content increased over the duration of the experiment due to the increasing difference in vegetation water content between the soybean and corn fields (an increase in range of 1.88 kg/m^2 from June 25 to July 11). Also, the July 10 rainfall event decreased the satellite-scale soil temperature from 30.08 C (0-1 cm volumetric soil moisture of $0.19 \text{ cm}^3/\text{cm}^3$) to 20.67 C (0-1 cm volumetric layer soil moisture of $0.34 \text{ cm}^3/\text{cm}^3$). Similarly, a decrease in brightness temperature was observed in all channels

from July 9 to July 10, a mean decrease of 7.31 K. Also, scattered rainfall increased the range and standard deviation of observed T_B in all channels during these days (e.g., the range and standard deviation of observed AMSR-E and PSR horizontally polarized 10.7 GHz T_B increased 6.14 K, 1.08 K, and 1.47 K, 0.47 K respectively from July 10 to July 11). Despite a large difference in spatial resolution of the two instruments, changes in vegetation water content and soil moisture had similar effects on the brightness temperature observed by both aircraft and satellite instruments.

3.1 AMSR-E observations

Both the forward modeling and the soil moisture retrieval algorithm are based on microwave radiative transfer. In the forward modeling, the T_B at a specific frequency and polarization is determined using observed soil moisture in conjunction with soil and vegetation parameters. Soil moisture retrieval uses observations of T_B in an iterative optimization technique that yields soil moisture by minimizing the difference between the computed and observed horizontally-polarized brightness temperatures. The value of estimated (retrieved) soil moisture is that which achieves a convergence of the observed and computed brightness temperatures.

Estimates of surface reflectivity are calculated from the Fresnel equations, using a semi-empirical formulation to characterize a rough surface from the height parameter h and polarization mixing parameter Q . These parameters are based on the soil surface height standard deviation and microwave wavelength. Vegetation scattering is dependent on vegetation opacity and is represented in the model as a single scattering layer above the emitting soil surface. The opacity is related to the vegetation water content w_c ,

by:

$$\tau_c = \frac{bw_c}{\cos \theta}$$

where θ is the incidence angle and the parameter b is approximately proportional to frequency and depends weakly on vegetation type and canopy structure at low frequencies. The brightness temperature T_{BP} at the top of the vegetation layer is calculated as a function of the soil brightness temperature and reflectivity with the addition of vegetation opacity τ_c , vegetation single-scattering albedo ω_p , and vegetation effective temperature T_{ce} :

$$T_{BP} = T_s (1 - r_p) e^{-\tau_c} + T_{ce} (1 - \omega) (1 - e^{-\tau_c}) (1 + r_p e^{-\tau_c})$$

where p is polarization and T_s is the effective soil temperature. For simplicity, T_{ce} values were taken from the 2 m elevation air temperature data provided by the Natural Resources Conservation Service (NRCS) Soil Climate Analysis Network (SCAN) site located within the study area during the hour of the AMSR-E overpass.

Considering the frequency (10.7 GHz) used and high levels of the vegetation water content observed, AMSR-E performed remarkably well during the experiment. A reasonable correlation of observed AMSR-E 10.7 GHz T_B with measured satellite-scale 0-1 cm volumetric soil moisture was found during the study. An R^2 of 0.41 was calculated for the horizontally-polarized channel and an R^2 value of 0.46 was calculated for the vertical channel. The increase in soil moisture throughout the study resulted in an overall decrease in T_B of 21 K. However, it is apparent that the large number of dry ($< 0.1 \text{ cm}^3/\text{cm}^3$) days had a significant impact on the correlation.

A comparison of the observed and forward modeled AMSR-E horizontally-polarized 10.7 GHz T_B gave an R^2 value of 0.53. The model simulated brightness temperatures gave lower than expected values of brightness temperature. The range of the estimated brightness temperatures was ~ 25 K compared to the observed brightness temperature range of ~ 15 K. The larger range of estimated brightness temperatures is possibly an artifact of the nonlinear relationship of the soil dielectric constant and moisture content at dry conditions⁸⁾. The dielectric constant gradient can also influence the thermal sampling depth⁹⁾. It is reasonable to assume that model errors related to thermal sampling depth are exacerbated by the extremely dry conditions observed during the initial days of SMEX02. The thermal sampling depth is the depth of the soil that contributes to the observed and modeled microwave brightness temperatures. This value is known to be dynamic and dependant on soil type, soil moisture, and climatic conditions. To this end, the depth from which the radiation originates can be overestimated in dry conditions and underestimated in wet conditions, resulting in a larger range of estimated values. Therefore, these differences must be considered when comparing soil moisture estimated in this way with in situ observations.

The influence of hydrometeorological conditions on the estimated and observed signals is further explored in Figure 1. The estimated 10.7 GHz horizontally-polarized T_B agrees well with the observed 10.7 GHz horizontally polarized T_B for the first part of the experiment, June 25th to July 4th. After July 4th, the observed T_B and estimated T_B appear to be less correlated. The estimated H-polarization T_B decreases at a faster rate (287 K to 264 K) from July 4th to July 7th than the observed H-polarization T_B (282 K to 278 K). These days corresponded to an increase in satellite-scale volumetric soil moisture (0.12-0.26 cm³/cm³).

From Fig. 1 the discrepancy between simulated and observed H-pol T_B occurs mostly from July 4th/6th onwards, when the SMEX02 domain is dominated by more damp conditions resulting from widespread precipitation events on these days.

One explanation for these differences is that the model does not properly account for the vegetation or temperature effects of open versus closed canopies during these days and therefore results in a greater dynamic range. Also, even though the microwave emission model was calibrated for the SMEX02 domain, vegetation and albedo coefficients are static in the model. It is likely that oversimplification of vegetation within the model led to brightness temperature estimation error. As shown in¹⁰, when using the same microwave emission model, even a slight underestimation of vegetation scattering can have a significant increase on modeled brightness temperature at 10 GHz.

3.2 PSR C/X observations

Results of PSR C/X at satellite-scale were consistent with the AMSR-E findings. Comparison of the satellite-scale horizontally-polarized PSR C/X data with 0-1 cm volumetric soil moisture resulted in R^2 correlation of 0.69. The observed satellite-scale PSR C/X 10.7 GHz T_B decreased nearly 18 K from a change in volumetric soil moisture range of $0.32 \text{ cm}^3/\text{cm}^3$. As with the observed AMSR-E T_B , the PSR C/X T_B had a better agreement during wetter conditions than drier conditions. A strong correlation ($R^2 = 0.81$) between estimated and observed satellite-scale PSR C/X 10.7 GHz brightness temperatures was observed. Estimated brightness temperature is biased by up to 10 K for some areas, i.e., under-estimation at lower values of T_B and over-estimation at higher values of T_B . Similar results were seen when

comparing the PSR C/X 7.3 GHz modeled and observed brightness temperatures; $R^2 = 0.84$ (not shown).

A time series of PSR C/X observed and estimated brightness temperatures is shown in Figure 2. The estimated vertical and horizontally polarized brightness temperatures were higher during June 25th through July 7th than July 8th through 12th. Drier regions resulted in an overestimation of brightness temperature in both the horizontal and vertical channels; the opposite was true for brightness temperatures below 278 K (wetter regions). After the July 11th rainfall, drier conditions were captured by both the observed and estimated 10.7 GHz brightness temperatures, as shown by an increase of ~1 K observed and ~6 K estimated.

3.3 Comparison of AMSR-E and PSR C/X observations

The observed AMSR-E brightness temperatures and PSR C/X satellite-scale brightness temperatures were shown to be relatively well correlated ($R^2=0.83$), with more scatter observed during the drier days/regions. As mentioned in section 3.2, it is possible that the non-linear relation is the result of non-uniform precipitation events and/or non-uniform drying patterns over the SMEX02 domain. Such events would increase the heterogeneity in soil moisture within the SMEX02 region during the dry days of the study. However, the statistics of the observed AMSR-E and PSR C/X 10.7 GHz channels are conflicting. The AMSR-E observations actually became more varied while the PSR C/X 2.3 km brightness temperatures converged. A scaling issue is not expected because the two instruments behave similarly at satellite-scale (see Figures 1 and 2). This is rather an artifact of radiometric averaging of the larger AMSR-E footprint. The finer PSR C/X footprints reflect a lower degree of sub-pixel variability.

However, considering the differences in spatial resolution and time of observation of the two instruments, the correlation is quite good.

3.4 Soil moisture estimation

The reliability of the soil moisture retrieval algorithm is highly dependent on the correlation of observed brightness temperatures with surface parameters and accuracy of the modeled emission. As expected from forward model comparisons, predictions were better for the wetter regions/days of the study. In all cases, the moisture retrieval algorithm had difficulty estimating lower volumetric soil moisture values ($<0.1 \text{ cm}^3/\text{cm}^3$), particularly from June 25th to July 4th when the volumetric soil moisture in the 0-1 cm layer was below $0.04 \text{ cm}^3/\text{cm}^3$ in many fields. Results are reflected in the retrieved soil moisture statistics; an R^2 of 0.74 and an RMS error of $0.10 \text{ cm}^3/\text{cm}^3$ were calculated for PSR C/X applied retrievals, and an R^2 of 0.45 and an RMS error of $0.07 \text{ cm}^3/\text{cm}^3$ were calculated for the AMSR-E applied retrievals. The model parameters characterizing vegetation structure and soil roughness had a greater impact on the modeled brightness in dry areas and on dry days. Hence, in extremely dry soils the influence of h , Q , w_c , and T_s on the modeled emission is exaggerated, resulting in a bias of estimated soil moisture. Biases of $-0.09 \text{ cm}^3/\text{cm}^3$ and $-0.07 \text{ cm}^3/\text{cm}^3$ volumetric soil moisture were calculated for the satellite-scale soil moisture estimates from AMSR-E and PSR C/X, respectively. These statistics indicate that the disparities between observed and estimated soil moisture are less likely due to poor instrument performance, and rather to other sources such as field sampling time lag or errors in model parameterization. Although reflecting a bias with observed volumetric soil moisture, the estimated soil

moisture values from each instrument gave significant agreement, with a correlation coefficient of 0.97.

To demonstrate the value of AMSR-E brightness temperatures for retrieving soil moisture with improved model characterization, AMSR-E brightness temperature observations were applied to the soil moisture retrieval algorithm over the wetter regions/days of the SMEX02 domain. Figure 3 shows the AMSR-E 10.7 GHz satellite-scale estimates over the SMEX02 regions with volumetric soil moisture content greater than $0.1 \text{ cm}^3/\text{cm}^3$. The explained variance over the damp conditions is $R^2=0.87$.

4. Conclusions and Discussion

Results demonstrated that the observed and modeled brightness temperatures accurately reflected the soil moisture variability during the SMEX02 campaign. Changes in satellite-scale volumetric soil moisture over the region were observed by the PSR C/X satellite-scale and AMSR-E 10.7 GHz brightness temperatures, R^2 values of 0.69, and 0.41 respectively with in situ soil moisture measurements. Comparison of AMSR-E and PSR C/X observed brightness temperatures ($R^2=0.83$ at 10.7 GHz H-polarization) provided a useful analysis of multi-scale soil moisture observations. Overall, the PSR C/X instrument was seen to have a higher correlation with soil moisture.

This study demonstrates reasonable ($R^2=0.67$, $\text{RMS}=0.07$) soil moisture estimates can be achieved using AMSR-E X-band data over the SMEX02 region. An upscaling of PSR C/X brightness temperatures to satellite-scale show agreement with the AMSR-E retrieved soil moisture. The PSR C/X applied retrievals resulted in correlations with observed satellite-scale 0-1 cm volumetric soil moisture

($R^2=0.74$, $RMS=0.10 \text{ cm}^3/\text{cm}^3$). Retrieval accuracy with the AMSR-E applied brightness temperatures was sufficiently better ($R^2=0.87$) in areas of moisture content greater than $0.1 \text{ cm}^3/\text{cm}^3$. Distinct biases over extremely dry soils demonstrate exaggerated effects of modeled parameters in those regions. For dry regions ($m_v < 0.1 \text{ cm}^3/\text{cm}^3$) the modeled brightness was not dominated by the moisture signal, but by other variables such as soil temperature and roughness. These forward modeled errors certainly impacted the soil moisture retrievals.

Results suggest that AMSR-E can provide large-scale estimates of soil moisture in regions with low levels of vegetation and that these estimates are consistent with findings across scales (i.e., field, airborne). This work supports previous SMEX02 soil moisture remote sensing studies and provides a unique framework for investigating important issues such as sub-pixel heterogeneity, frequency, and scale on satellite-scale soil moisture remote sensing. The given results are relevant to future satellite missions involving soil moisture remote sensing such as the Soil Moisture and Ocean Salinity (SMOS) mission and highlights a need for more efficient methods of soil moisture estimation in agricultural (corn canopy) regions using microwave data.

References

- 1) T. Schmugge and T. J. Jackson : Mapping Surface Soil-Moisture with Microwave Radiometers, *Meteorology and Atmospheric Physics*, 54(1-4), pp. 213-223, 1994.
- 2) J. D. Bolten, V. Lakshmi, and E. G. Njoku : Soil moisture retrieval using the passive/active L- and S-band radar/radiometer, *IEEE Transactions on Geoscience and Remote Sensing*, 41(12), pp. 2792-2801, 2003.
- 3) M. F. McCabe, B. H. Gao, and E. F. Wood : An evaluation of AMSR-E derived soil moisture retrievals using ground based, airborne and ancillary data during SMEX02, *Journal of Hydrometeorology*, 6(6), pp. 864-877, 2004.
- 4) R. Bindlish, T. J. Jackson, A. J. Gasiewski, M. Klein, and E.G. Njoku : Soil moisture mapping and AMSR-E validation using the PSR in SMEX02, *Remote Sensing of Environment*, 103, pp. 127-139, 2006.
- 5) T. J. Jackson, D. Y. Chen, M. Cosh, F. Q. Li, M. Anderson, C. Walthall, P. Doriaswamy, and E. R. Hunt : Vegetation water content mapping using Landsat data derived normalized difference water index for corn and soybeans, *Remote Sensing of Environment*, 92(4), pp. 475-482, 2004.
- 6) T. Kawanishi, T. Sezai, Y. Ito, K. Imaoka, T. Takeshima, Y. Ishido, A. Shibata, M. Miura, H. Inahata, and R. W. Spencer : The Advanced Microwave Scanning Radiometer for the Earth Observing System (AMSR-E), NASDA's contribution to the EOS for global energy and water cycle studies, *IEEE Transactions on Geoscience and Remote Sensing*, 41(2), pp. 84-194, 2003.

- 7) T. J. Jackson, A. J. Gasiewski, A. Oldak, M. Klein, E. G. Njoku, A. Yevgrafov, S. Christiani, and R. Bindlish : Soil moisture retrieval using the C-band polarimetric scanning radiometer during the Southern Great Plains 1999 Experiment, IEEE Transactions on Geoscience and Remote Sensing, 40(10), pp. 2151-2161, 2002.
- 8) J. R. Wang and T. J. Schmugge : An empirical model for the complex dielectric permittivity of soil as a function of water content, IEEE Transactions on Geoscience and Remote Sensing, GE-23, pp. 35-46, 1980.
- 9) T. J. Schmugge and B. J. Choudhury : A comparison of radiative transfer models for predicting the microwave emission from soils, Radio Science, 16, pp. 927-938, 1981.
- 10) E. G. Njoku and L. Li : Retrieval of land surface parameters using passive microwave measurements at 6-18 GHz, IEEE Transactions on Geoscience and Remote Sensing, 37(1), pp. 79-93, 1999.

Figures and Tables:

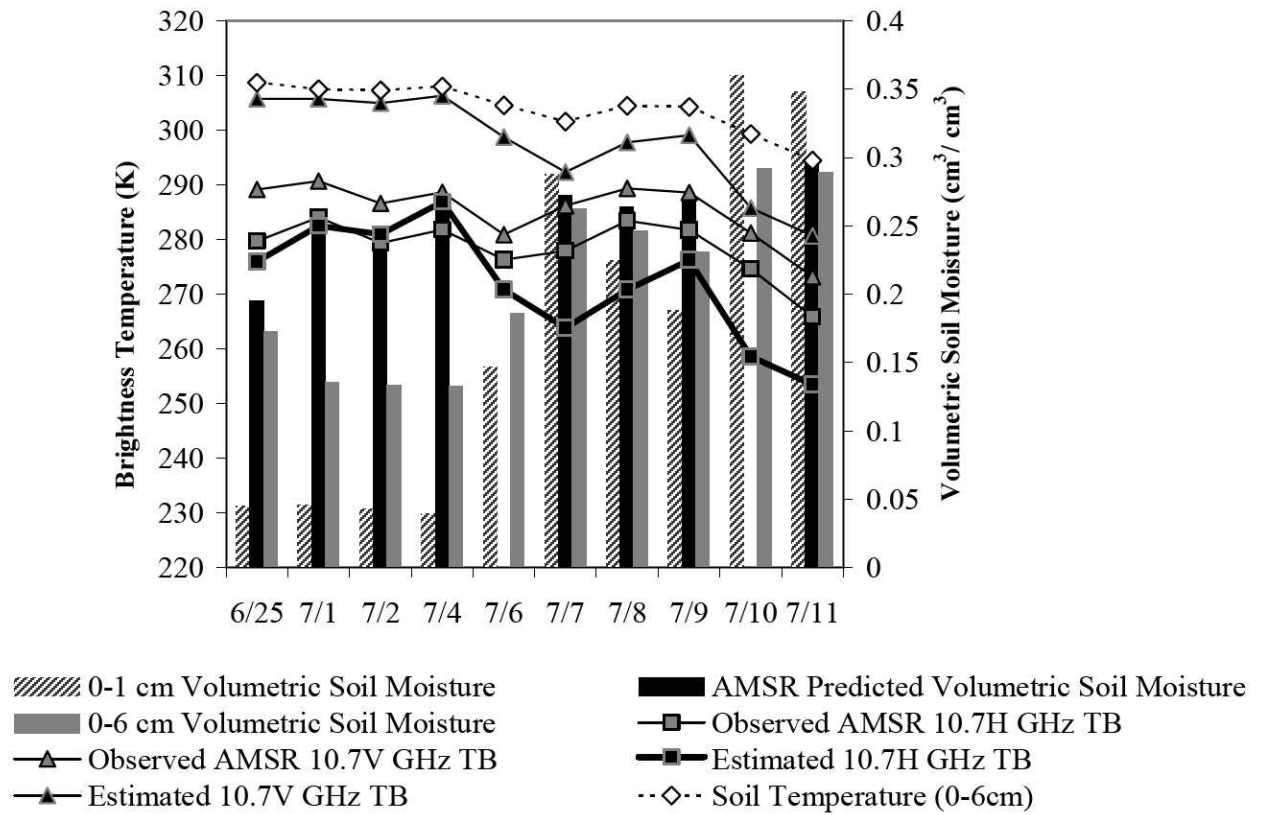


Fig. 1. Time-series of estimated and observed AMSR 10.7 GHz H- and V- polarized T_B with *in situ* soil moisture and temperature.

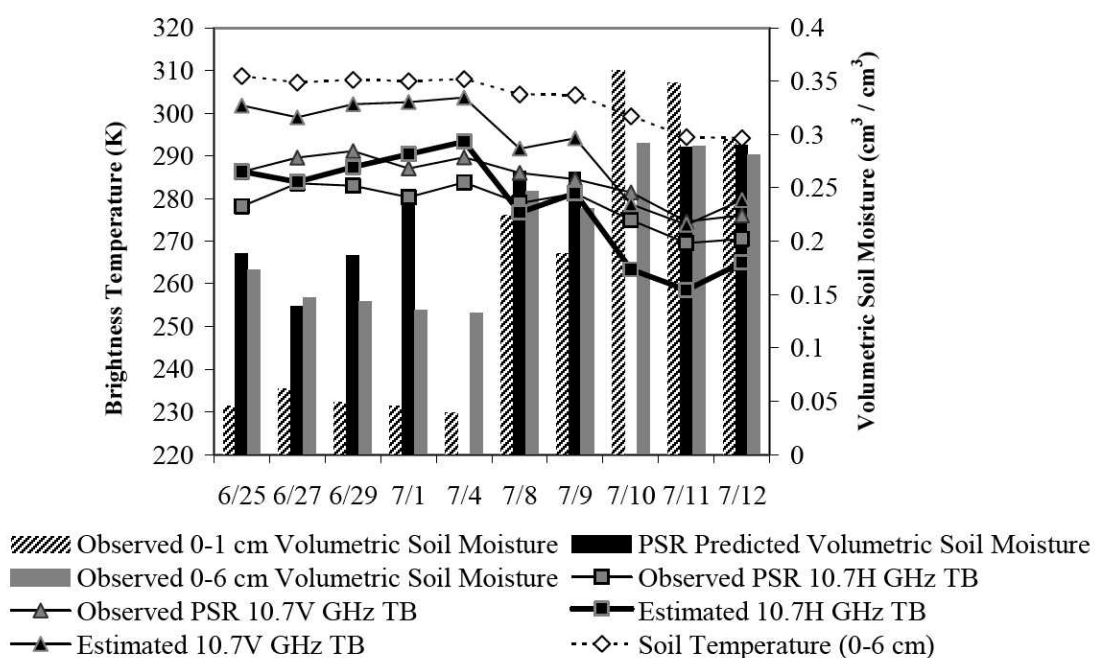


Fig. 2. Time-series of estimated and observed satellite-scale PSR 10.7 GHz H- and V-polarized T_B with *in situ* soil moisture and temperature.

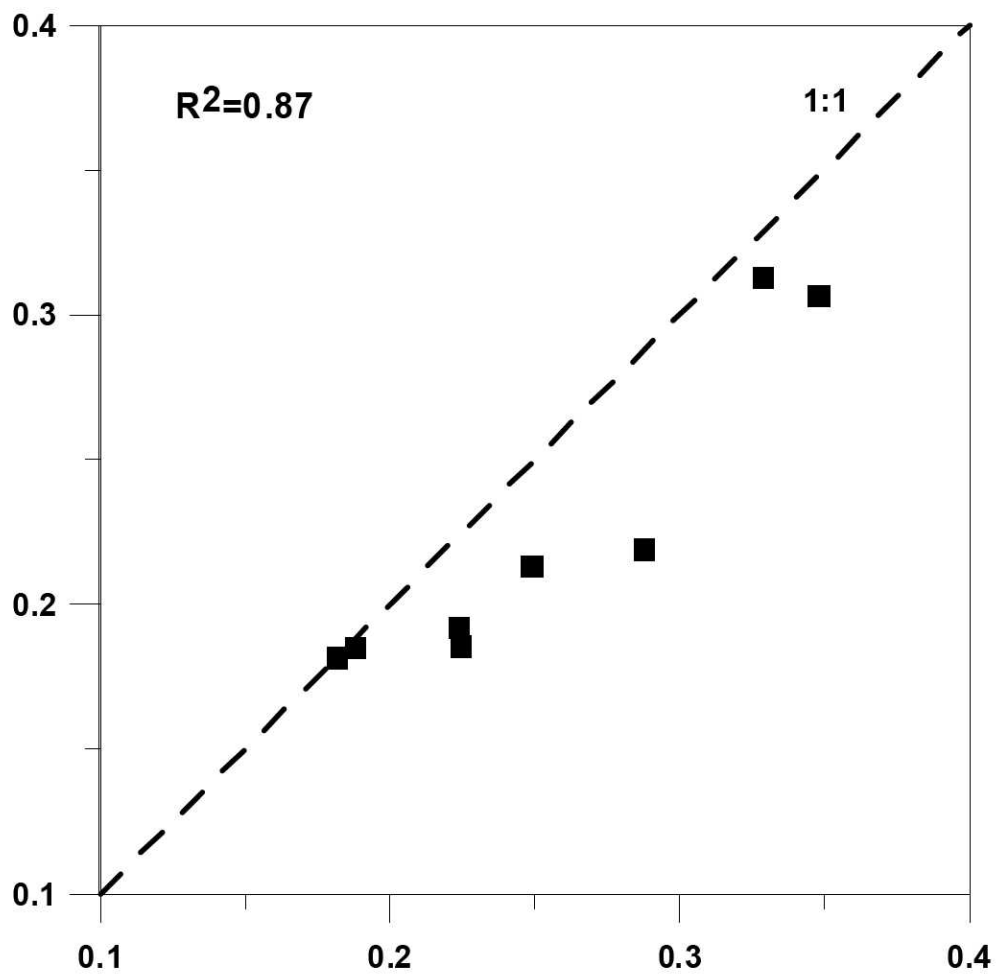


Fig. 3. AMSR 10.7 GHz estimated satellite-scale soil moisture for fields having greater than 0.10 cm³/cm³ volumetric soil moisture.

Observed T_B	m_v 0-1 cm	m_v 0-6 cm
	R^2	R^2
AMSR 10.7 GHz H	0.409	0.372
AMSR 10.7 GHz V	0.462	0.389
AMSR 6.9 GHz H	0.218	0.157
AMSR 6.9 GHz V	0.279	0.212
PSR 10.7 GHz H	0.691	0.695
PSR 10.7 GHz V	0.767	0.752
PSR 7.3 GHz H	0.701	0.694
PSR 7.3 GHz V	0.800	0.769

Table 1. Statistics for the observed T_B and regional in situ volumetric soil moisture.